

Phase Diffusion in Localized Spatio-Temporal Amplitude Chaos

Glen D. Granzow and Hermann Riecke

Department of Engineering Sciences and Applied Mathematics, Northwestern University, Evanston, IL 60208, USA

We present numerical simulations of coupled Ginzburg-Landau equations describing parametrically excited waves which reveal persistent dynamics due to the occurrence of phase slips in sequential pairs, with the second phase slip quickly following and negating the first. Of particular interest are solutions where these double phase slips occur irregularly in space and time within a spatially localized region. An effective phase diffusion equation utilizing the long term phase conservation of the solution explains the localization of this new form of amplitude chaos.

November 13, 2018

Spatio-temporal chaos poses one of the important challenges in the investigation of spatially extended dynamical systems. A central question regarding these systems concerns the characterization and classification of the chaotic states. This has been studied most extensively for chaotic traveling waves in one dimension within the framework of a complex Ginzburg Landau equation. There, two different dynamic regimes have been identified, a phase-chaotic regime and an amplitude-chaotic regime [1–4]. The latter is characterized by the occurrence of phase slips during which the amplitude of the wave goes to zero and the total phase of the system changes by 2π , i.e. a wavelength is inserted or eliminated. In the phase-chaotic regime essentially no phase slips occur [2,4]. This chaotic regime can be described by an equation for the phase of the wave alone [5]. In the amplitude-chaotic regime this is not possible since the phase equation breaks down during phase slips.

In this letter we present a different class of spatio-temporal chaos, which we have identified in one-dimensional simulations of parametrically excited waves. The observed chaos is characterized by the occurrence of *double phase slips* which effectively preserve the total phase. Thus, although the phase description breaks down during each of the phase slips, the long-time dynamics can still be described by an *effective* phase equation. The second striking result of our simulations is the localization of spatio-temporal chaos in a part of the homogeneous system. That is, there are solutions that include a spatial region, bounded by quiescent regions on each side, in which the dynamics are irregular in space and time. Experimentally, similar phenomena have been observed in Taylor vortex flow [6], Rayleigh-Benard convection [7], and parametrically excited surface waves [8]. So far, the localization mechanism in these systems is only poorly understood.

For the system of equations discussed in this letter (which model parametrically excited waves) the localization can be understood using the effective phase equation. We confirm the validity of this approach by explicitly determining the effective phase diffusion coefficient. The short-scale chaotic dynamics amount to fluctuations on the large scales captured by the phase description. They may therefore introduce a noise term in the effective phase diffusion equation similar to that arising in the Kardar-Parisi-Zhang equation [9], which describes the large-scale behavior of spatio-temporal chaos in the Kuramoto-Sivashinsky equation [10–12], the leading-order phase equation for the complex Ginzburg Landau equation [5].

Parametrically excited waves arise quite generally in systems exhibiting weakly damped modes that are oscillatory in both space and time, when these modes are forced at twice their natural frequency [13,14]. Faraday’s experiment in which surface waves are formed on a liquid in a vertically oscillated container is perhaps the best known example (e.g. [15,16,8]). Other examples are parametrically forced spin waves [17,18], and traveling waves in electroconvection [19] and in Taylor Dean flow [20]. For small forcing amplitude, these systems can be modeled by a pair of coupled Ginzburg-Landau equations [13,14],

$$\partial_T A + s\partial_X A = d\partial_X^2 A + aA + bB + cA(|A|^2 + |B|^2) + gA|B|^2 \quad (1)$$

$$\partial_T B - s\partial_X B = d^*\partial_X^2 B + a^*B + bA + c^*B(|A|^2 + |B|^2) + g^*B|A|^2. \quad (2)$$

The dependent variables A and B are complex, and represent amplitudes of left and right traveling waves which are summed together to yield the solution of the underlying system:

$$u(x, t) = \epsilon A(X, T)e^{i(q_c x - \frac{\omega_c}{2}t)} + \epsilon B(X, T)e^{i(q_c x + \frac{\omega_c}{2}t)} + c.c. + O(\epsilon^2). \quad (3)$$

They vary on slow time and space scales, $T = \epsilon^2 t$ and $X = \epsilon x$ respectively. The coefficient b of the linear coupling term gives the amplitude of the periodic forcing.

Stationary solutions to equations (1,2) of the form $A = A_0 e^{iqX}$, $B = B_0 e^{iqX}$ (where A_0 and B_0 are complex constants) include those where the amplitudes of A and B are equal, corresponding to standing waves in the underlying system which are phase-locked to the external forcing [13,14]. In this letter we discuss results of numerical simulations of the ensuing dynamics when the standing waves are perturbed. These simulations were

performed using a Fourier spectral method in space (periodic boundary conditions) and a fourth order Runge-Kutta/integrating-factor scheme in time.

The linear stability diagram for the standing-wave solution of equations (1,2) with the parameters chosen for this study is shown in figure 1 [21]. For small values of b ($b = 0.1$, say) solutions to equations (1,2) behave like those of a single real Ginzburg-Landau equation; given an initial condition slightly to the right of the Eckhaus stable region, the solution will undergo a phase slip which reduces the wave number and moves the solution into the stable region (e.g. [22]). This single-phase-slip behavior is shown in figure 2a. For larger values of b however ($b = 0.6$, say), the behavior of the solution is markedly different; given an initial condition slightly to the right of the Eckhaus stable region, the solution undergoes a phase slip which reduces the average wave number but a short time later undergoes a second phase slip at essentially the same location which restores the wavenumber to its original value. This double phase slip, shown in figure 2b, causes the solution to remain in the Eckhaus unstable region, thus allowing persistent dynamics.

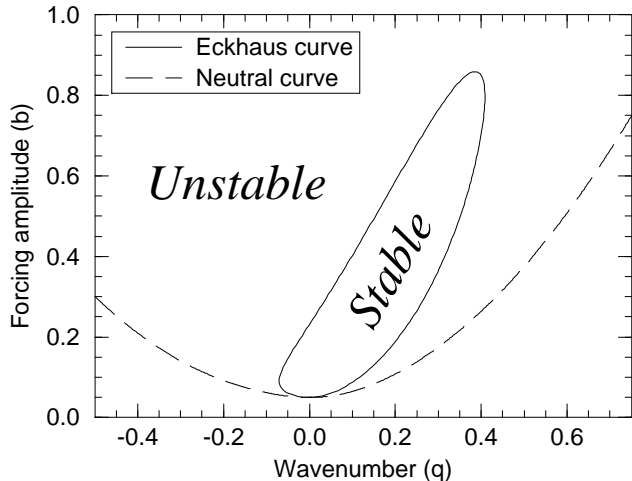


FIG. 1. Stability diagram for parametrically driven standing waves with $a = -0.05$, $c = -1 + 4i$, $d = 1 + 0.5i$, $s = 0.2$, $g = -1 - 12i$.

Simulations of a small system (5 wavelengths long) show that the complexity of the ensuing dynamics is dependent on the distance of the initial condition from the Eckhaus stable region. Very close to the Eckhaus curve simple periodic solutions occur. In these solutions double phase slips occur at only one location in space, periodically in time. Further to the right, away from the Eckhaus stable regime the simple periodic solutions lose stability to more complicated periodic solutions and these more complicated periodic solutions in turn lose stability to solutions where the double phase slips occur irregularly in time and space over the entire domain. This irregular occurrence of double phase slips is a form of spatio-temporal amplitude chaos. Starting with an initial condition far to the right of the Eckhaus curve, single

phase slips occur which reduce the wavenumber and thus move the system to the left, into a region where a stationary, periodic, or chaotic solution is stable.

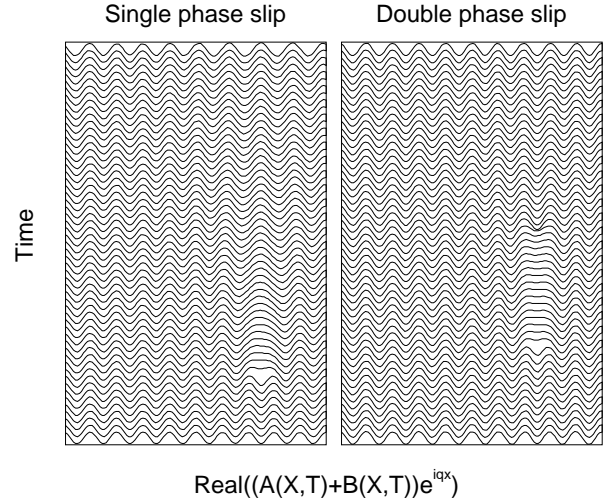


FIG. 2. Space-time diagrams illustrating a) single phase slip observed for small values of the forcing amplitude (e.g. $b = 0.1$), and b) double phase slip observed for larger values of the forcing amplitude (e.g. $b = 0.6$). Other parameters as in figure 1.

In larger systems (here 47 wavelengths long) and at intermediate distances from the Eckhaus stable regime we find that the chaotic activity need not spread through the whole system. Instead, double phase slips occur only in a spatially confined region. This is illustrated in figure 3 which shows the location in space and time of double phase slips. Here an initial maximum in the local wavenumber triggers a double phase slip which subsequently causes more double phase slips in the neighborhood of the first. These double phase slips occur irregularly in space and time within a region whose size initially grows but remains bounded in space. Outside of this region the solution remains stationary (i.e. in physical space there are regular, periodic standing waves, cf.(3)).

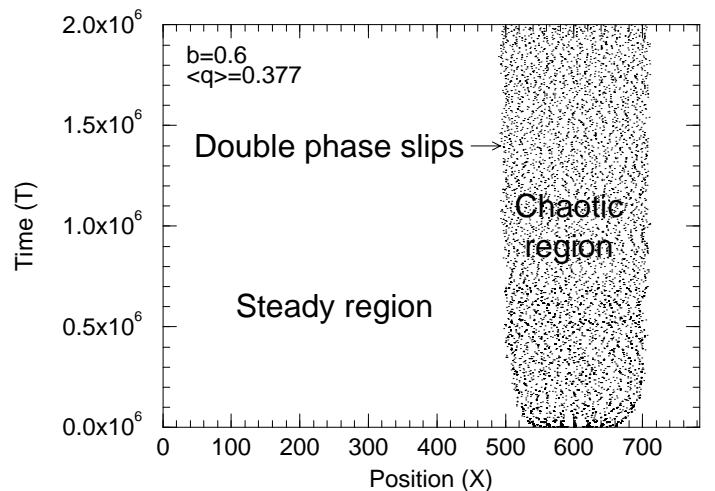


FIG. 3. Space-time diagram showing each double phase slip as a single dot. The spatio-temporal chaos is confined to a small part of the system ($b = 0.6$, other parameters as in figure 1; the averaged effective wavenumber is $\langle q \rangle = 0.377$).

To understand the localization mechanism we turn to the phase diffusion equation

$$\partial_T \phi(X, T) = D(q) \partial_X^2 \phi(X, T), \quad (4)$$

which describes the slow evolution of the phase ϕ of a steady pattern. Equation (4) is nonlinear through the dependence of the diffusion coefficient on the wave number $q \equiv \partial_X \phi$. The use of the phase equation is motivated by the observation that the temporally averaged local wavenumber is larger in the chaotic region than in the steady region. The state shown in figure 3 can therefore be considered to consist of two domains, one with large and one with small wavenumber. It has been shown previously [23,21,24] that such domain structures can be stable if the diffusion coefficient $D(q)$ is negative (indicating an unstable solution) only over a small range of wavenumbers q . Initial conditions with a uniform wavenumber in this range will then evolve to a structure consisting of domains in which the local wavenumber lies in either of the two adjacent ranges of stable wavenumbers. The stability of the domain structure is due to the conservation of the total phase and the instability of the state with the corresponding uniform wavenumber.

As a basic condition for this mechanism to explain the localization shown in figure 3 the phase description has to be valid, requiring in particular that the phase is conserved. Across individual phase slips the phase is not conserved and the phase equation (4) breaks down. However, across a *double* phase slip the phase *is* conserved. On sufficiently long time scales we therefore expect an *effective* phase equation to be appropriate. Reflexion symmetry in space but not in time suggests an equation of the form (4) with the phase and the diffusion coefficient replaced by an effective phase $\hat{\phi}$ and an effective diffusion coefficient $\hat{D}(\hat{q})$. To substantiate this claim we determine $\hat{D}(\hat{q})$ by measuring the (diffusive) response of the extended chaotic state to a localized time-periodic forcing. Specifically, we include a spatially local, time-periodic advection term in equations (1,2) giving:

$$\partial_T A + (v + s) \partial_X A = d \partial_X^2 A + aA + bB + cA(|A|^2 + |B|^2) + gA|B|^2 \quad (5)$$

$$\partial_T B + (v - s) \partial_X B = d^* \partial_X^2 B + a^* B + bA + c^* B(|A|^2 + |B|^2) + g^* B|A|^2 \quad (6)$$

$$\text{with } v = \begin{cases} v_0 \sin(\omega T) & \text{for } X_1 \leq X \leq X_2 \\ 0 & \text{otherwise.} \end{cases}$$

For relatively small values of ω_0 formerly stationary solutions start to drift within the region $X_1 \leq X \leq X_2$, periodically reversing their direction according to the sign of v . For the regions $X < X_1$, and $X > X_2$ the situation resembles an imposed boundary condition at $X = X_1$,

and $X = X_2$ at which the phase of the solution varies sinusoidally. This is similar to the approach used in experiments on turbulent Taylor vortex flow wherein an endcap was moved sinusoidally [25].

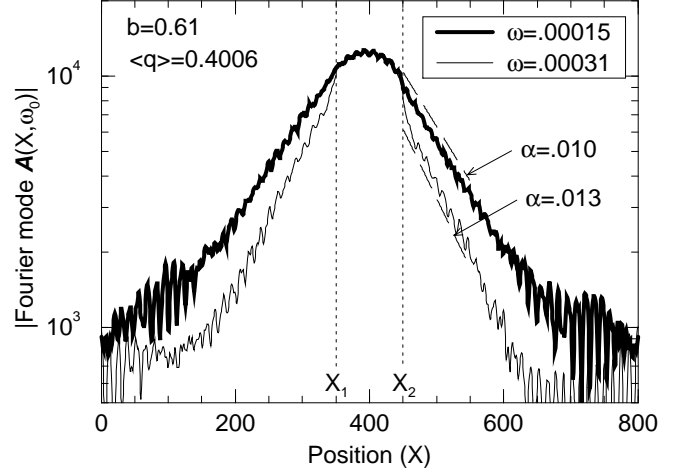


FIG. 4. Decay of the magnitude of the coefficient of the time Fourier transform of A corresponding to the frequency ω_0 in the localized advection term v in equations (5,6), for two different values of ω_0 ($b = 0.61$, other parameters as in figure 1; the averaged effective wavenumber is $\langle q \rangle = 0.4006$).

The solution to the diffusion equation $\partial_t \hat{\phi}(X, t) = \hat{D} \partial_X^2 \hat{\phi}(X, t)$ for $X > X_2$, with $\hat{\phi}(X_2, t) = \hat{\phi}_0 \sin(\omega_0 t)$, is

$$\hat{\phi}(X, t) = \hat{\phi}_0 e^{-\alpha(X-X_2)} \sin(\omega_0 t - \beta(X-X_2)) \quad (7)$$

$$\text{where } \alpha = \beta = \sqrt{\frac{\omega_0}{2\hat{D}}}. \quad (8)$$

If the phase of the solution A in the region $X > X_2$ obeys this relationship, then the magnitude of the Fourier mode $\mathcal{A}(X, \omega_0)$ corresponding to the frequency ω_0 will decay exponentially in space as X increases from X_2 . Figure 4 shows that this exponential behavior is realized in our simulations. Note that the data for figure 4 is from a simulation that produced double phase slips irregularly in space and time over the entire domain (not localized chaos). The phase slips introduce noise which can be seen in figure 4. In order to reduce the effect of this noise and extract a reliable decay rate α , the Fourier integral has been extended over many periods (88) of the function $v(X, T)$ in the advection term in equations (5,6). Equation (8) shows that for diffusive behavior the decay rate α is proportional to $\omega_0^{1/2}$. The ratio of the slopes of the curves in figure 4 are consistent with this diffusive scaling. We conclude that the dynamics are indeed diffusive and show in figure 5 the diffusion coefficient as a function of the wavenumber. The solid curve shows the analytical phase diffusion coefficient for the stationary solution [21] while the triangles show the effective phase diffusion coefficient for the chaotic solution as measured using the decay rate α of the Fourier mode $\mathcal{A}(X, \omega)$ for $\omega = \omega_0$ and

$\omega = -\omega_0$ for $X > X_2$ and $X < X_1$ as described above. Despite the scatter in the data it is clear that $\hat{D}(\hat{q})$ decreases with decreasing \hat{q} and presumably goes to zero at a wavenumber for which the diffusion coefficient of the nonchaotic state is still negative as shown by the dashed line. Thus the system is diffusively unstable over a range of wavenumbers, and initial conditions with an average wavenumber in this range will evolve into domains of chaotic and nonchaotic waves.

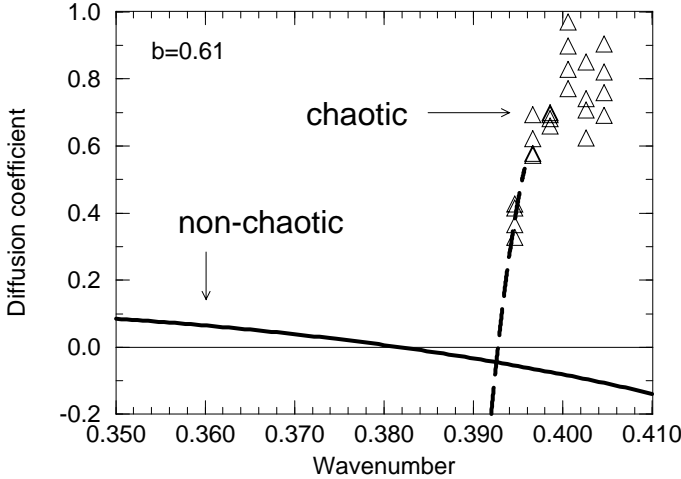


FIG. 5. Analytical phase diffusion coefficient for the stationary solution (solid line) and effective diffusion coefficient for the chaotic solution (triangles represent numerical results, the dashed line is the presumed extension of these results). ($b = 0.61$, other parameters as in figure 1.)

Figure 5 suggests that the chaotic activity should not disappear homogeneously if the average wavenumber is decreased towards the stable regime. Instead, the homogeneously chaotic state should split up into chaotic and stationary domains in which the local wavenumber is in the respective stable regimes ($D > 0$ and $\hat{D} > 0$). This is indeed found in our numerical simulations.

To summarize, we have presented numerical simulations of spatio-temporal chaos in parametrically excited standing waves. We have demonstrated that despite the fact that the chaos must be classified as amplitude chaos its large-scale features can nevertheless be described by an effective phase equation. The reason for this surprising result lies in the fact that the phase slips always come in pairs such that the total phase is effectively conserved. We have determined the effective diffusion coefficient. This allowed us to identify a simple mechanism for the localization of the spatio-temporally chaotic state which is related to the occurrence of domain structures and zig-zags in steady patterns [23,21,24,26].

So far we have not identified a particular physical system which exhibits the behavior described here. It is natural to suspect that the closing of the Eckhaus curve (cf. figure 1) is related to the occurrence of double phase slips. If that should be the case, parametric driving of waves which are Benjamin-Feir unstable in the absence of

any forcing should be a good candidate for this behavior. Within the framework of the coupled Ginzburg-Landau equations (1,2) these waves become unstable near the band center when forced sufficiently strongly [27]. Depending on the sign of certain nonlinear coefficients this indicates instability at all wavenumbers and a closing of the Eckhaus curve.

We would like to thank J. Eggers for helpful discussions. This work was supported by the United States Department of Energy through grant DE-FG02-92ER14303.

-
- [1] B. Shraiman *et al.*, *Physica D* **57**, 241 (1992).
 - [2] D. Egolf and H. Greenside, *Phys. Rev. Lett.* **74**, 1751 (1995).
 - [3] H. Chaté and P. Manneville, *Physica A* **224**, 348 (1996).
 - [4] P. Manneville and H. Chaté, *Physica D* (1996).
 - [5] Y. Kuramoto, *Prog. Theor. Phys. Suppl.* **64**, 346 (1978).
 - [6] B. Baxter and C. Andereck, *Phys. Rev. Lett.* **57**, 3046 (1986).
 - [7] S. Ciliberto and M. Rubio, *Phys. Rev. Lett.* **58**, 2652 (1987).
 - [8] A. Kudrolli and J. Gollub, submitted to PRL .
 - [9] M. Kardar, G. Parisi, and Y. Zhang, *Phys. Rev. Lett.* **56**, 889 (1986).
 - [10] V. Yakhot, *Phys. Rev. A* **24**, 642 (1981).
 - [11] S. Zaleski, *Physica D* **34**, 427 (1989).
 - [12] C. Jayaprakash, F. Hayot, and R. Pandit, *Phys. Rev. Lett.* **71**, 12 (1993).
 - [13] H. Riecke, J. Crawford, and E. Knobloch, *Phys. Rev. Lett.* **61**, 1942 (1988).
 - [14] D. Walgraef, *Europhys. Lett.* **7**, 485 (1988).
 - [15] M. Cross and P. Hohenberg, *Rev. Mod. Phys.* **65**, 851 (1993).
 - [16] N. Tufillaro, R. Ramshankar, and J. Gollub, *Phys. Rev. Lett.* **62**, 422 (1989).
 - [17] H. Suhl, *J. Phys. Chem. Solids* **1**, 209 (1957).
 - [18] F. Elmer, *Phys. Rev. Lett.* **70**, 2028 (1993).
 - [19] I. Rehberg *et al.*, *Phys. Rev. Lett.* **61**, 2449 (1988).
 - [20] S. Tennakoon, C. Andereck, J. Hegseth, and H. Riecke, in preparation .
 - [21] H. Riecke, *Europhys. Lett.* **11**, 213 (1990).
 - [22] L. Kramer, H. Schober, and W. Zimmermann, *Physica D* **31**, 212 (1988).
 - [23] H. Brand and R. Deissler, *Phys. Rev. Lett.* **63**, 508 (1989).
 - [24] D. Raitt and H. Riecke, *Physica D* **82**, 79 (1995).
 - [25] M. Wu, C. Andereck, and H. Brand, *Europhys. Lett.* **19**, 587 (1992).
 - [26] E. Bodenschatz *et al.*, in *The Geometry of Non-Equilibrium*, edited by P. Coulet and P. Huerre (Plenum, New York, 1990), p. 111.
 - [27] H. Riecke, in *Nonlinear Evolution of Spatio-Temporal Structures in Dissipative Continuous Systems*, edited by F. Busse and L. Kramer (Plenum Press, New York, 1990), pp. 437-444.